

Electronic Supplementary Information

Paddlewheel-type and half-paddlewheel-type diruthenium(II,II) complexes with 1,8-naphthyridine-2-carboxylate

Yusuke Kataoka,^{*a} Nozomi Tada,^a Naoki Masamori,^a Natsumi Yano,^a Chikako Moriyoshi,^b Makoto Handa^{*a}

^a Department of Chemistry, Graduate School of Natural Science and Technology, Shimane University

^b Graduate School of Advanced Science and Engineering, Hiroshima University,

Contents

Scheme S1. Molecular structures of (a) *cis*-2:2- and (b) *trans*-2:2-arrangements of $[\text{Ru}_2(\mu\text{-npc})_2(\text{O}_2\text{CR})_2]$.

Fig. S1. Observed and simulated ESI-TOF-MS spectra of **1**.

Fig. S2. ^1H NMR spectrum of **1** in $\text{DMSO}-d_6$.

Fig. S3. Observed and simulated ESI-TOF-MS spectra of **2**.

Fig. S4. Observed and simulated ESI-TOF-MS spectra of **3**.

Fig. S5. ^1H NMR spectrum of **2** in $\text{DMSO}-d_6$.

Fig. S6. ^1H NMR spectrum of **3** in $\text{DMSO}-d_6$.

Table S1. Selected bond lengths (\AA) and angles ($^\circ$) of crystal structure of **1**.

Table S2. Selected bond lengths (\AA) and angles ($^\circ$) of crystal structure of **2**.

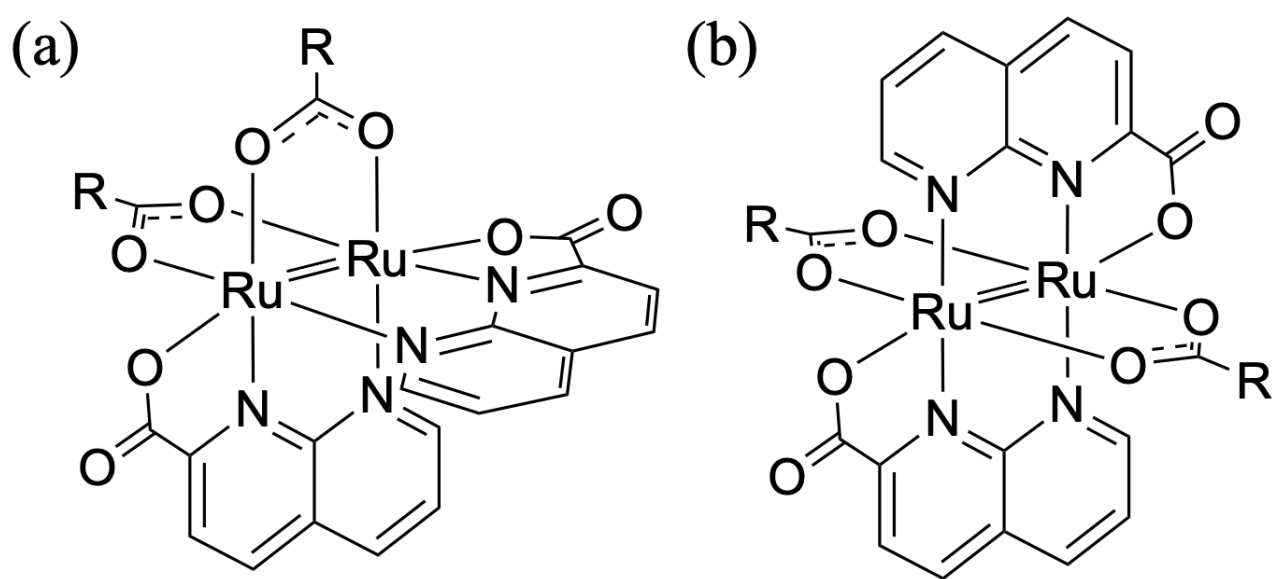
Table S3. Selected bond lengths (\AA) and angles ($^\circ$) of crystal structure of **3**.

Table S4. Averaged bond lengths (\AA) and angles ($^\circ$) of optimized geometries of **1-3**.

Table S5. Table S5. Result of TDDFT calculation of **1** (H and L indicate the HOMO and LUMO, respectively).

Table S6. Table S5. Result of TDDFT calculation of **2** (H and L indicate the HOMO and LUMO, respectively).

Table S7. Table S5. Result of TDDFT calculation of **3** (H and L indicate the HOMO and LUMO, respectively).



Scheme S1. Molecular structures of (a) *cis*-2:2- and (b) *trans*-2:2-arrangements of $[\text{Ru}_2(\mu\text{-npc})_2(\text{O}_2\text{CR})_2]$.

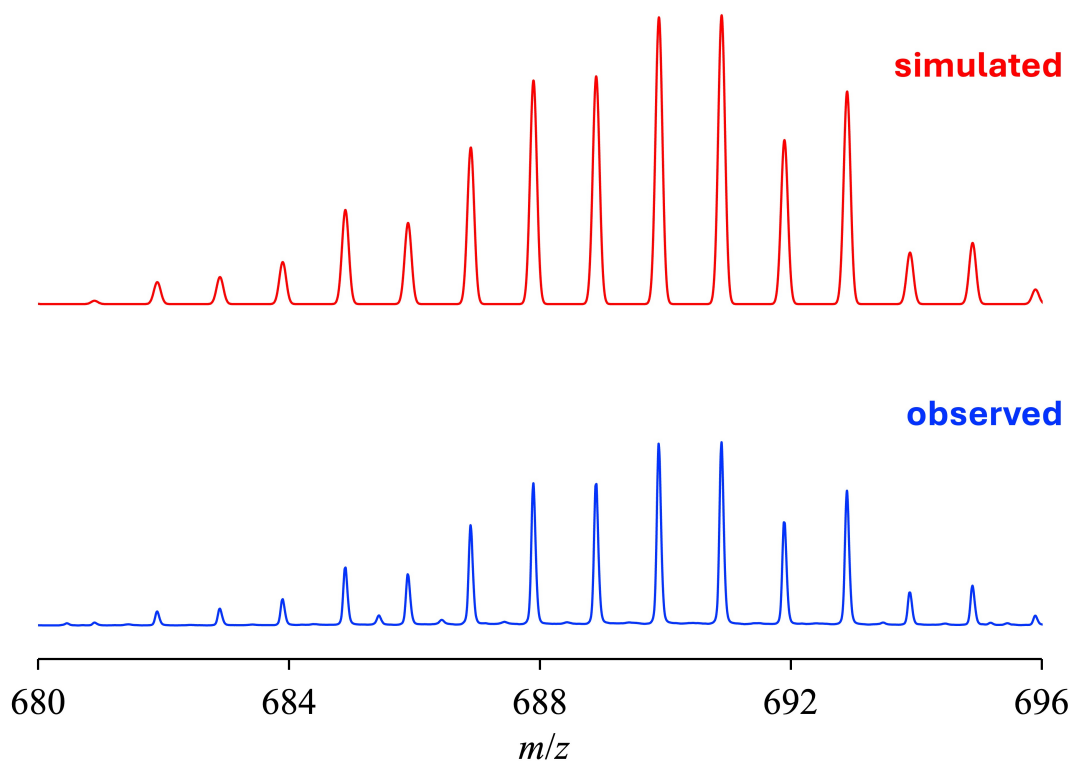


Fig. S1. Observed and simulated ESI-TOF-MS spectra of **1**.

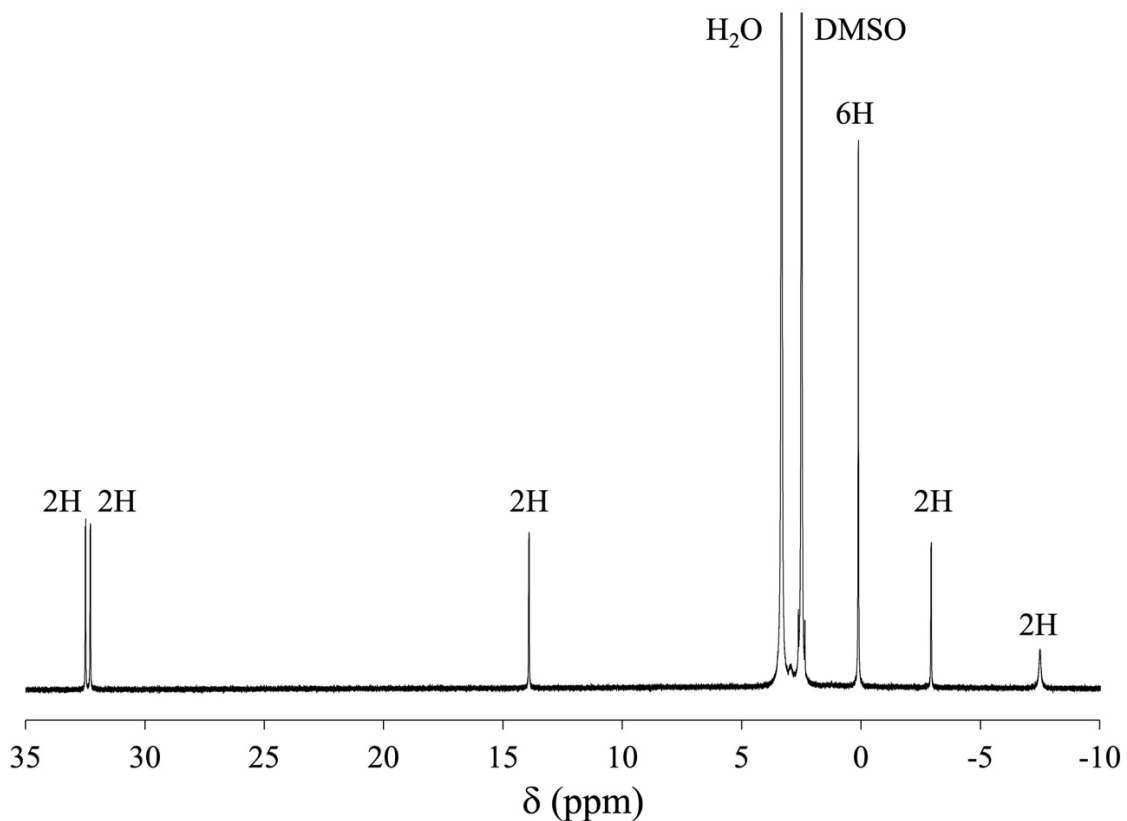


Fig. S2. ^1H NMR spectrum of **1** in $\text{DMSO}-d_6$.

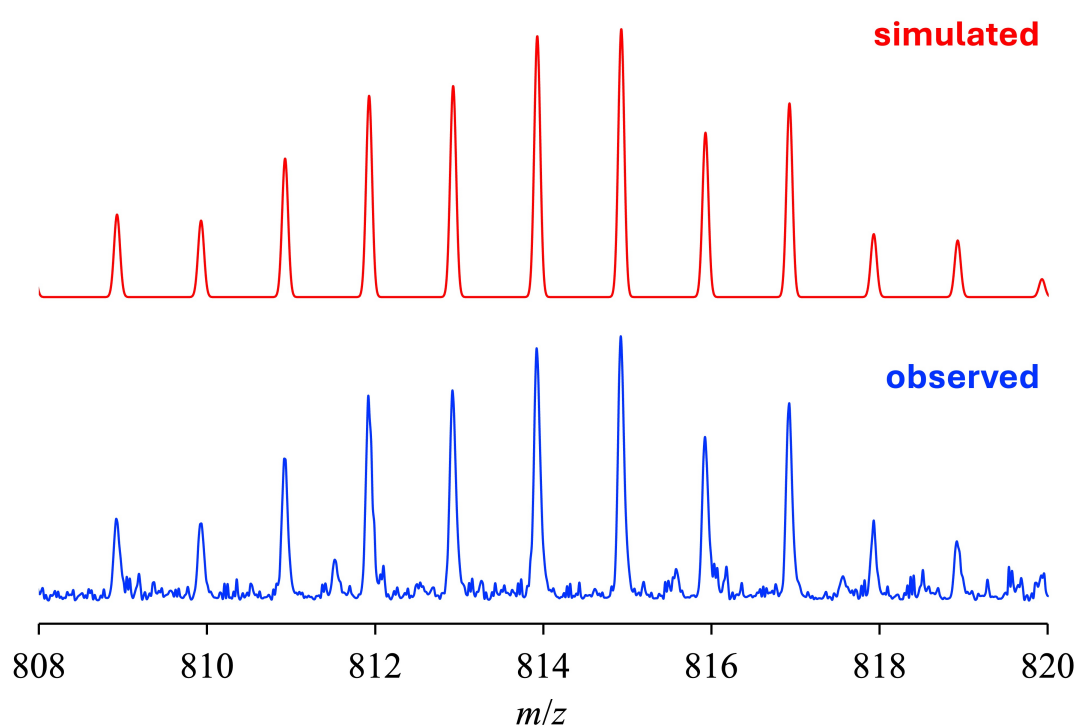


Fig. S3. Observed and simulated ESI-TOF-MS spectra of 2.

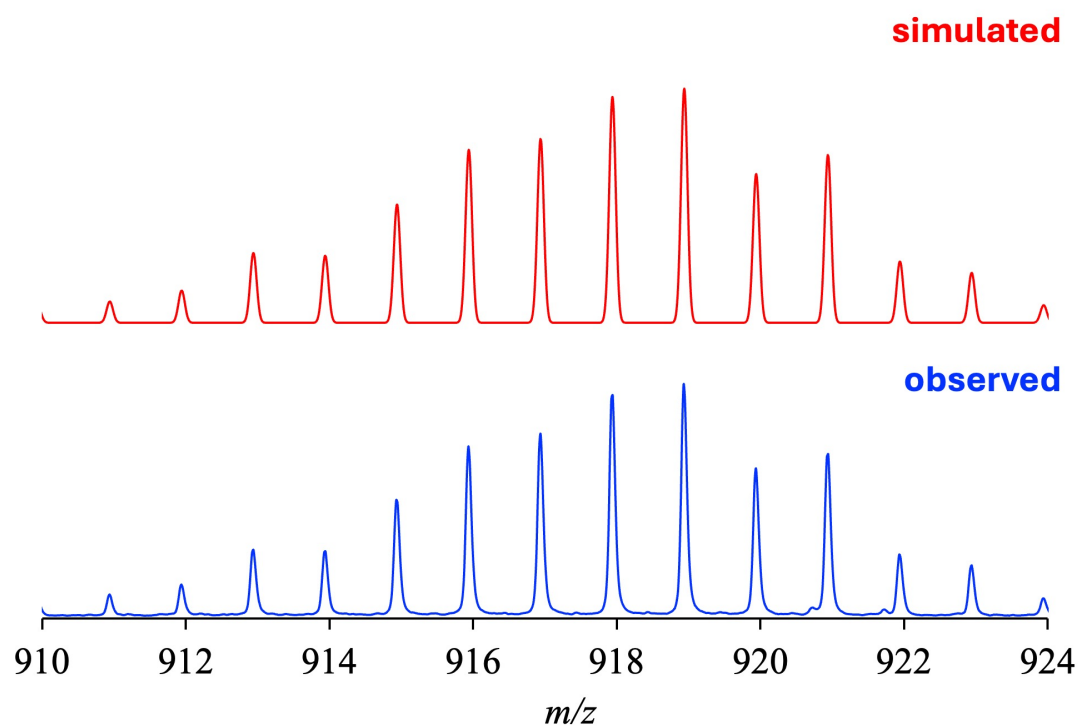


Fig. S4. Observed and simulated ESI-TOF-MS spectra of 3.

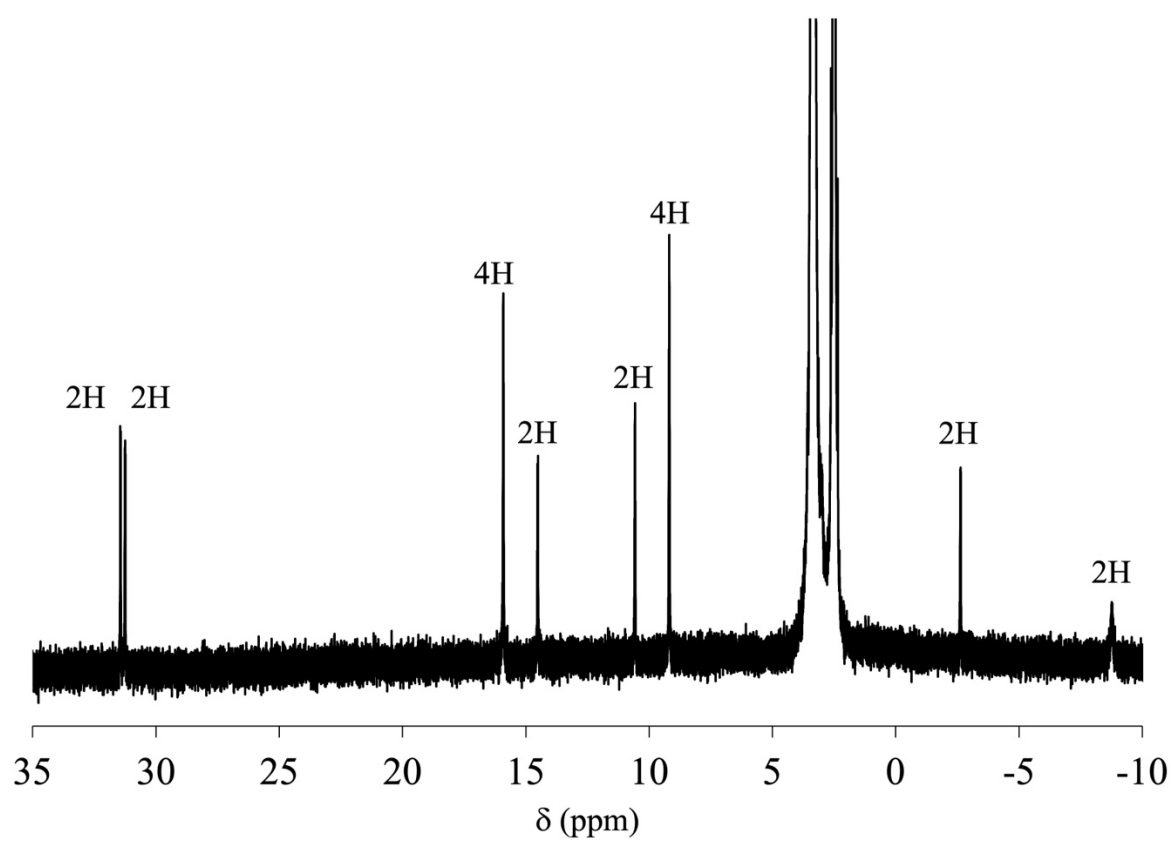


Fig. S5. ^1H NMR spectrum of **2** in $\text{DMSO}-d_6$.

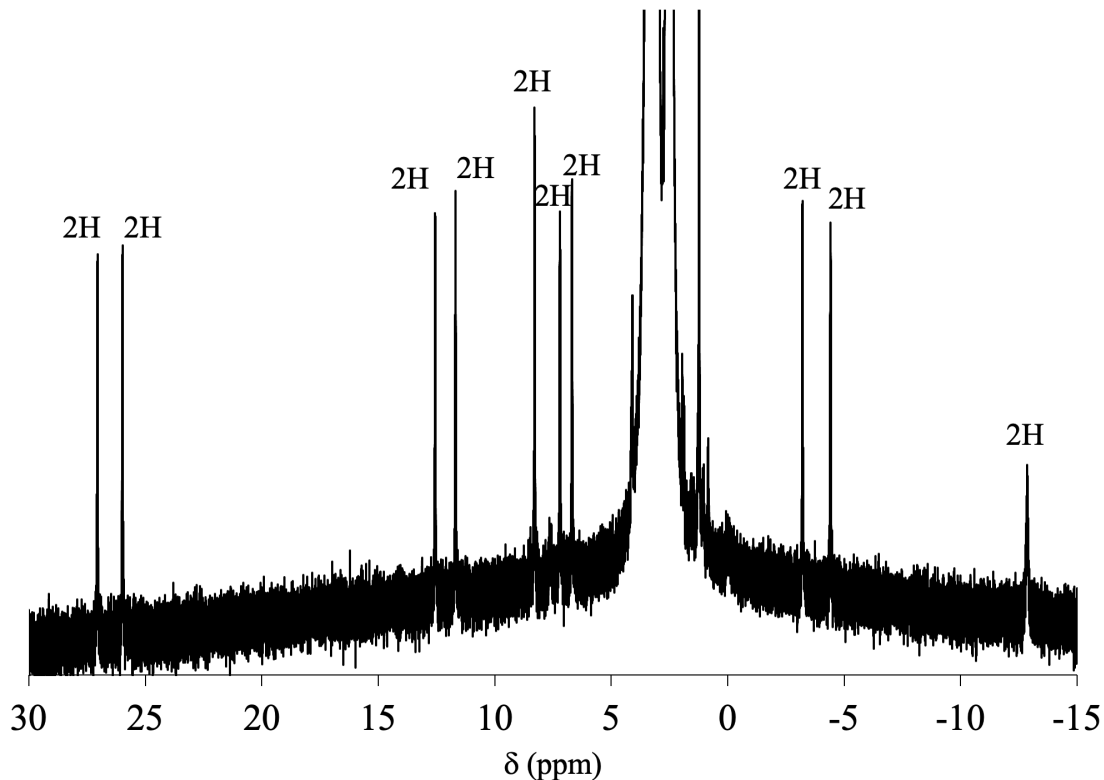


Fig. S6. ^1H NMR spectrum of **3** in $\text{DMSO}-d_6$.

Table S1. Selected bond lengths (Å) and angles (°) of **1**.

bond lengths (Å)			
Ru1-Ru1'	2.2893(4)	C9-O1	1.267(4)
Ru1-N1	2.039(2)	C9-O2	1.234(4)
Ru1-N2'	2.063(3)	C10-O3	1.250(5)
Ru1-O3	2.082(2)	C10-O4	1.289(5)
Ru1-O4'	2.069(2)	C5-N1	1.364(3)
Ru1-O1	2.243(2)	C5-N2	1.384(4)
bond angles (°)			
Ru1- Ru1'-N1'	90.17(6)	Ru1- Ru1'-O1'	165.87(6)
Ru1- Ru1'-N2'	90.81(7)	N1-Ru1-O1	76.00(9)
Ru1- Ru1'-O3'	88.13(6)	O3-C10-O4	124.1(3)
Ru1- Ru1'-O4	90.40(7)	N1-C5-N2	115.9(2)

Table S2. Selected bond lengths (Å) and angles (°) of **2**.

bond lengths (Å)			
Ru1-Ru1'	2.2834(6)	C9-O1	1.286(6)
Ru1-N1	2.044(3)	C9-O2	1.230(6)
Ru1-N2'	2.073(3)	C10-O3	1.262(5)
Ru1-O3	2.049(3)	C10-O4	1.276(5)
Ru1-O4'	2.085(3)	C5-N1	1.360(5)
Ru1-O1	2.225(3)	C5-N2	1.367(6)
bond angles (°)			
Ru1- Ru1'-N1'	90.87(10)	Ru1- Ru1'-O1'	167.52(8)
Ru1- Ru1'-N2'	90.10(10)	N1-Ru1-O1	76.80(13)
Ru1- Ru1'-O3'	90.68(8)	O3-C10-O4	124.0(3)
Ru1- Ru1'-O4	88.14(8)	N1-C5-N2	116.5(3)

Table S3. Selected bond lengths (Å) and angles (°) of **3**.

bond lengths (Å)			
Ru1-Ru1'	2.3582(6)	C9-O1	1.249(8)
Ru1-N1	2.061(4)	C9-O2	1.236(8)
Ru1-N2'	2.078(3)	C18-O3	1.293(5)
Ru1-N3	2.101(4)	C18-O4	1.223(6)
Ru1-O3	2.034(3)	C5-N1	1.360(6)
Ru1-O1	2.200(3)	C5-N2	1.363(6)
bond angles (°)			
Ru1- Ru1'-N1'	87.98(11)	Ru1- Ru1'-O1	164.57(10)
Ru1- Ru1'-N2'	90.48(10)	N1-Ru1-O1	76.60(14)
Ru1- Ru1'-N3'	93.00(10)	N3-Ru1-O3	79.71(14)
Ru1- Ru1'-O3'	103.23(10)	N1-C5-N2	115.6(4)

Table S4. Averaged bond lengths (Å) and angles (°) of optimized geometries of **1-3**.

	1	2	3
Ru-Ru	2.318	2.318	2.415
Ru-N _(μ-npc)	2.091	2.090	2.106
Ru-O _(μ-npc)	2.256	2.255	2.245
Ru-O _(equatorial carboxylate)	2.099	2.096	—
Ru-N _(η²-npc)	—	—	2.145
Ru-O _(η²-npc)	—	—	2.044
Ru-Ru-N _(μ-npc)	90.17	90.18	88.68
Ru-Ru-O _(μ-npc)	164.64	164.63	163.04
Ru-Ru-O _(equatorial carboxylate)	89.00	89.01	—
Ru-Ru-O _(η²-npc)	—	—	102.96
Ru-Ru-N _(η²-npc)	—	—	96.66

Table S5. Result of TDDFT calculation of **1** (H and L indicate the HOMO and LUMO, respectively).

S _n	Wavelength (nm)	f	Major contributions	Band
3	775.5	0.0039	H-1(β) [σ(Ru ₂)] → L+2(β) [π*(Ru ₂)] (52%) H-1(β) [σ(Ru ₂)] → L+1(β) [π*(npc)] (22%) H-3(β) [π(Ru ₂)] → L+3(β) [π*(Ru ₂)] (14%)	A
4	764.2	0.0326	H(β) [δ*(Ru ₂)] → L(β) [π*(npc)] (80%)	
5	750.9	0.0075	H(β) [δ*(Ru ₂)] → L+1(β) [π*(npc)] (64%) H-2(α) [δ*(Ru ₂)] → L+1(α) [π*(npc)] (20%)	
12	611.7	0.0076	H-3(β) [π(Ru ₂)] → L+3(β) [π*(Ru ₂)] (45%) H-4(β) [π(Ru ₂)] → L+2(β) [π*(Ru ₂)] (19%) H-4(β) [π(Ru ₂)] → L+1(β) [π*(npc)] (10%)	B
14	583.1	0.0021	H-1(α) [π*(Ru ₂)] → L(α) [π*(npc)] (92%)	
15	563.5	0.1154	H-2(α) [δ*(Ru ₂)] → L(α) [π*(npc)] (80%) H(β) [δ*(Ru ₂)] → L(β) [π*(npc)] (11%)	
16	541.4	0.0047	H-4(β) [π(Ru ₂)] → L+3(β) [π*(Ru ₂)] (69%)	C
17	535.8	0.0102	H-4(β) [π(Ru ₂)] → L+2(β) [π*(Ru ₂)] (30%) H-3(β) [π(Ru ₂)] → L+3(β) [π*(Ru ₂)] (17%) H-4(β) [π(Ru ₂)] → L+1(β) [π*(npc)] (14%) H(α) [π*(Ru ₂)] → L+6(α) [σ*(Ru ₂)] (13%)	
18	515.4	0.0569	H-2(α) [δ*(Ru ₂)] → L+1(α) [π*(npc)] (52%) H(β) [δ*(Ru ₂)] → L+1(β) [π*(npc)] (15%)	
19	503.6	0.0058	H-1(β) [σ(Ru ₂)] → L(β) [π*(npc)] (88%)	

Table S6. Result of TDDFT calculation of **2** (H and L indicate the HOMO and LUMO, respectively).

S_n	Wavelength (nm)	f	Major contributions	Band
3	778.0	0.0030	H-1(β) [$\sigma(\text{Ru}_2)$] \rightarrow L+2(β) [$\pi^*(\text{Ru}_2)$] (47%) H-1(β) [$\sigma(\text{Ru}_2)$] \rightarrow L+1(β) [$\pi^*(\text{npc})$] (25%) H-3(β) [$\pi(\text{Ru}_2)$] \rightarrow L+3(β) [$\pi^*(\text{Ru}_2)$] (14%)	A
4	761.6	0.0334	H(β) [$\delta^*(\text{Ru}_2)$] \rightarrow L(β) [$\pi^*(\text{npc})$] (81%)	
5	748.9	0.0098	H(β) [$\delta^*(\text{Ru}_2)$] \rightarrow L+1(β) [$\pi^*(\text{npc})$] (44%) H(β) [$\delta^*(\text{Ru}_2)$] \rightarrow L+2(β) [$\pi^*(\text{Ru}_2)$] (28%) H-2(α) [$\delta^*(\text{Ru}_2)$] \rightarrow L+1(α) [$\pi^*(\text{npc})$] (20%)	
12	612.4	0.0068	H-3(β) [$\pi(\text{Ru}_2)$] \rightarrow L+3(β) [$\pi^*(\text{Ru}_2)$] (46%) H-4(β) [$\pi(\text{Ru}_2)$] \rightarrow L+2(β) [$\pi^*(\text{Ru}_2)$] (17%) H-4(β) [$\pi(\text{Ru}_2)$] \rightarrow L+1(β) [$\pi^*(\text{npc})$] (12%)	B
14	580.2	0.0017	H-1(α) [$\pi^*(\text{Ru}_2)$] \rightarrow L(α) [$\pi^*(\text{npc})$] (91%)	
15	562.3	0.1152	H-2(α) [$\delta^*(\text{Ru}_2)$] \rightarrow L(α) [$\pi^*(\text{npc})$] (79%) H(β) [$\delta^*(\text{Ru}_2)$] \rightarrow L(β) [$\pi^*(\text{npc})$] (11%)	
16	540.9	0.0061	H-4(β) [$\pi(\text{Ru}_2)$] \rightarrow L+3(β) [$\pi^*(\text{Ru}_2)$] (69%)	C
17	537.4	0.0092	H-4(β) [$\pi(\text{Ru}_2)$] \rightarrow L+2(β) [$\pi^*(\text{Ru}_2)$] (28%) H-4(β) [$\pi(\text{Ru}_2)$] \rightarrow L+1(β) [$\pi^*(\text{npc})$] (17%) H-3(β) [$\pi(\text{Ru}_2)$] \rightarrow L+3(β) [$\pi^*(\text{Ru}_2)$] (16%) H(α) [$\pi^*(\text{Ru}_2)$] \rightarrow L+8(α) [$\sigma^*(\text{Ru}_2)$] (12%),	
18	515.7	0.0792	H-2(α) [$\delta^*(\text{Ru}_2)$] \rightarrow L+1(α) [$\pi^*(\text{npc})$] (53%) H(β) [$\delta^*(\text{Ru}_2)$] \rightarrow L+1(β) [$\pi^*(\text{npc})$] (14%)	
19	502.4	0.0057	H-1(β) [$\sigma(\text{Ru}_2)$] \rightarrow L(β) [$\pi^*(\text{npc})$] (90%)	

Table S7. Result of TDDFT calculation of **3** (H and L indicate the HOMO and LUMO, respectively).

S _n	Wavelength (nm)	<i>f</i>	Major contributions	Band
6	701.3	0.0016	H(α) [$\pi^*(Ru_2)$] \rightarrow L+1(α) [$\pi^*(\mu\text{-}npc)$] (35%), H-3(β) [$\delta(Ru_2)$] \rightarrow L(β) [$\pi^*(Ru_2)/\pi^*(\eta^2\text{-}npc)$] (29%), H(β) [$\delta^*(Ru_2)$] \rightarrow L+4(β) [$\pi^*(Ru_2)$] (12%)	A'
9	666.5	0.0101	H-2(β) [$\pi(Ru_2)$] \rightarrow L+4(β) [$\pi^*(Ru_2)$] (36%), H-4(β) [$\pi(Ru_2)$] \rightarrow L(β) [$\pi^*(Ru_2)/\pi^*(\eta^2\text{-}npc)$] (18%)	
10	654.5	0.0186	H(β) [$\delta^*(Ru_2)$] \rightarrow L+1(β) [$\pi^*(\mu\text{-}npc)$] (76%), H-2(α) [$\delta^*(Ru_2)$] \rightarrow L(α) [$\pi^*(\mu\text{-}npc)$] (11%)	
11	653.1	0.0129	H(β) [$\delta^*(Ru_2)$] \rightarrow L+2(β) [$\pi^*(\mu\text{-}npc)$] (69%), H-2(α) [$\delta^*(Ru_2)$] \rightarrow L+1(α) [$\pi^*(\mu\text{-}npc)$] (21%)	
17	589.4	0.023	H-1(α) [$\pi^*(Ru_2)$] \rightarrow L+2(α) [$\pi^*(\eta^2\text{-}npc)$] (25%), H(α) [$\pi^*(Ru_2)$] \rightarrow L+8(α) [$\sigma^*(Ru_2)$] (10%)	B'
20	555.1	0.0028	H(β) [$\delta^*(Ru_2)$] \rightarrow L+3(β) [$\pi^*(\eta^2\text{-}npc)$] (62%), H-1(α) [$\pi^*(Ru_2)$] \rightarrow L+2(α) [$\pi^*(\eta^2\text{-}npc)$] (20%)	
24	523.1	0.0107	H(β) [$\delta^*(Ru_2)$] \rightarrow L+5(β) [$\pi^*(Ru_2)/\pi^*(\eta^2\text{-}npc)$] (59%), H(β) [$\delta^*(Ru_2)$] \rightarrow L(β) [$\pi^*(Ru_2)/\pi^*(\eta^2\text{-}npc)$] (17%)	
25	511.1	0.0473	H-2(α) [$\delta^*(Ru_2)$] \rightarrow L(α) [$\pi^*(\mu\text{-}npc)$] (53%), H-3(β) [$\delta(Ru_2)$] \rightarrow L+2(β) [$\pi^*(\mu\text{-}npc)$] (16%), H(β) [$\delta^*(Ru_2)$] \rightarrow L+1(β) [$\pi^*(\mu\text{-}npc)$] (11%)	C'
26	505.7	0.0467	H-3(β) [$\delta(Ru_2)$] \rightarrow L+2(β) [$\pi^*(\mu\text{-}npc)$] (30%), H(α) [$\pi^*(Ru_2)$] \rightarrow L+8(α) [$\sigma^*(Ru_2)$] (26%), H-2(α) [$\delta^*(Ru_2)$] \rightarrow L(α) [$\pi^*(\mu\text{-}npc)$] (24%)	
27	500.8	0.0924	H-1(β) [$\sigma(Ru_2)$] \rightarrow L+3(β) [$\pi^*(\eta^2\text{-}npc)$] (49%), H-1(α) [$\pi^*(Ru_2)$] \rightarrow L+3(α) [$\pi^*(\eta^2\text{-}npc)$] (23%), H-2(α) [$\delta^*(Ru_2)$] \rightarrow L+1(α) [$\pi^*(\mu\text{-}npc)$] (10%)	